

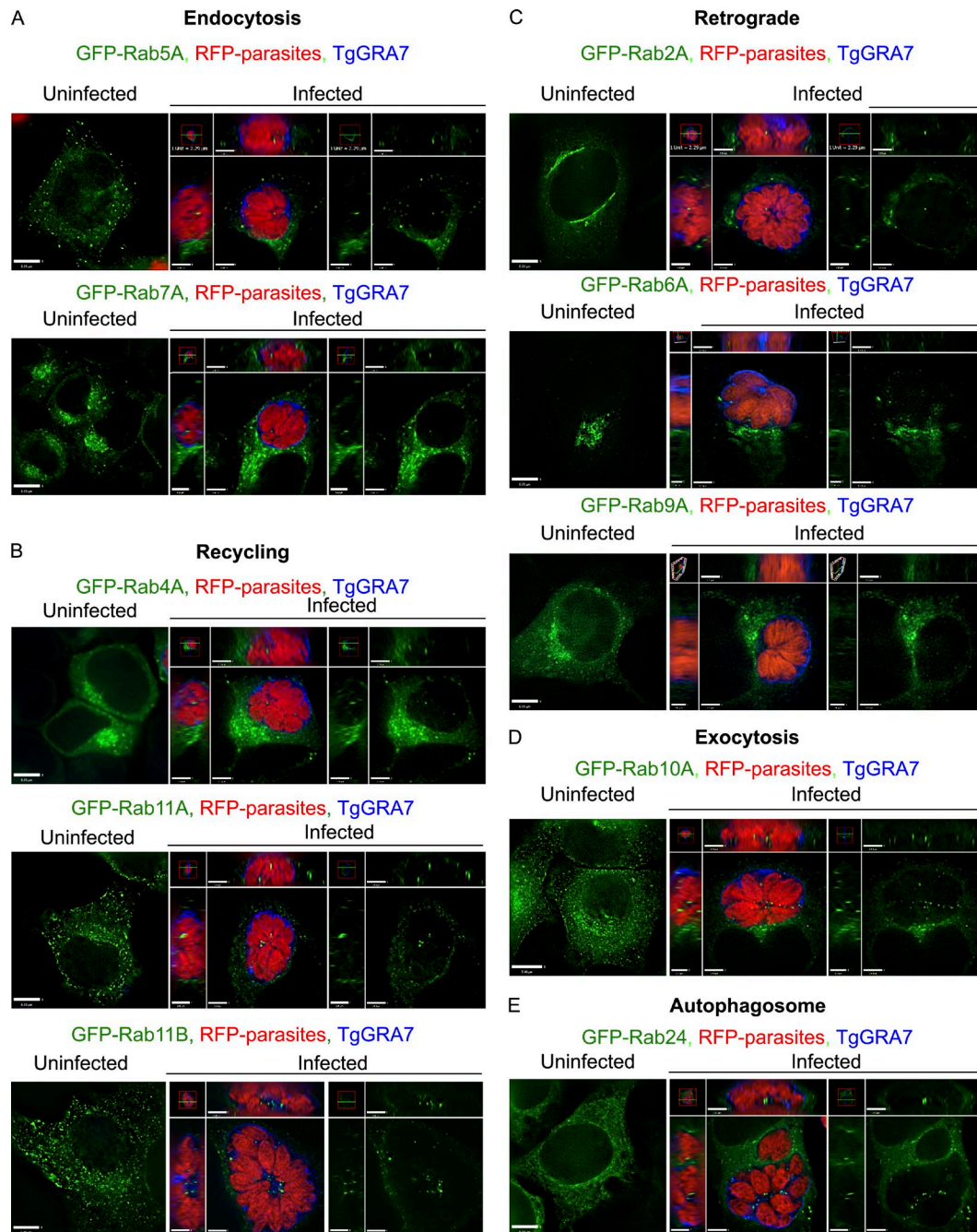
Romano et al., <https://doi.org/10.1083/jcb.201701108>

Figure S1. **Internalization of host GFP-Rab proteins from different host vesicular trafficking pathways.** (A–E) HeLa cells expressing host GFP-Rab constructs (green) involved in endocytosis (A), recycling (B), retrograde (C), exocytosis (D), and autophagosomal trafficking (E) were infected with RFP-RH for 24 h and immunostained for TgGRA7 (blue). Shown are an individual z-slice for uninfected cells and orthogonal views highlighting the PV. Bars: (A–C) 6 μ m; (A, orthogonal views for Rab5) 1.8 μ m; (A, orthogonal views for Rab7) 1.6 μ m; (B, orthogonal views) 1.7 μ m; (C, orthogonal views for Rab2) 1.8 μ m; (C, orthogonal views for Rab6) 1.5 μ m; (C, orthogonal views for Rab9) 1.6 μ m; (D) 7 μ m; (D, orthogonal views for Rab10) 1.6 μ m; (E) 6 μ m; (E, orthogonal views for Rab24) 1.7 μ m.

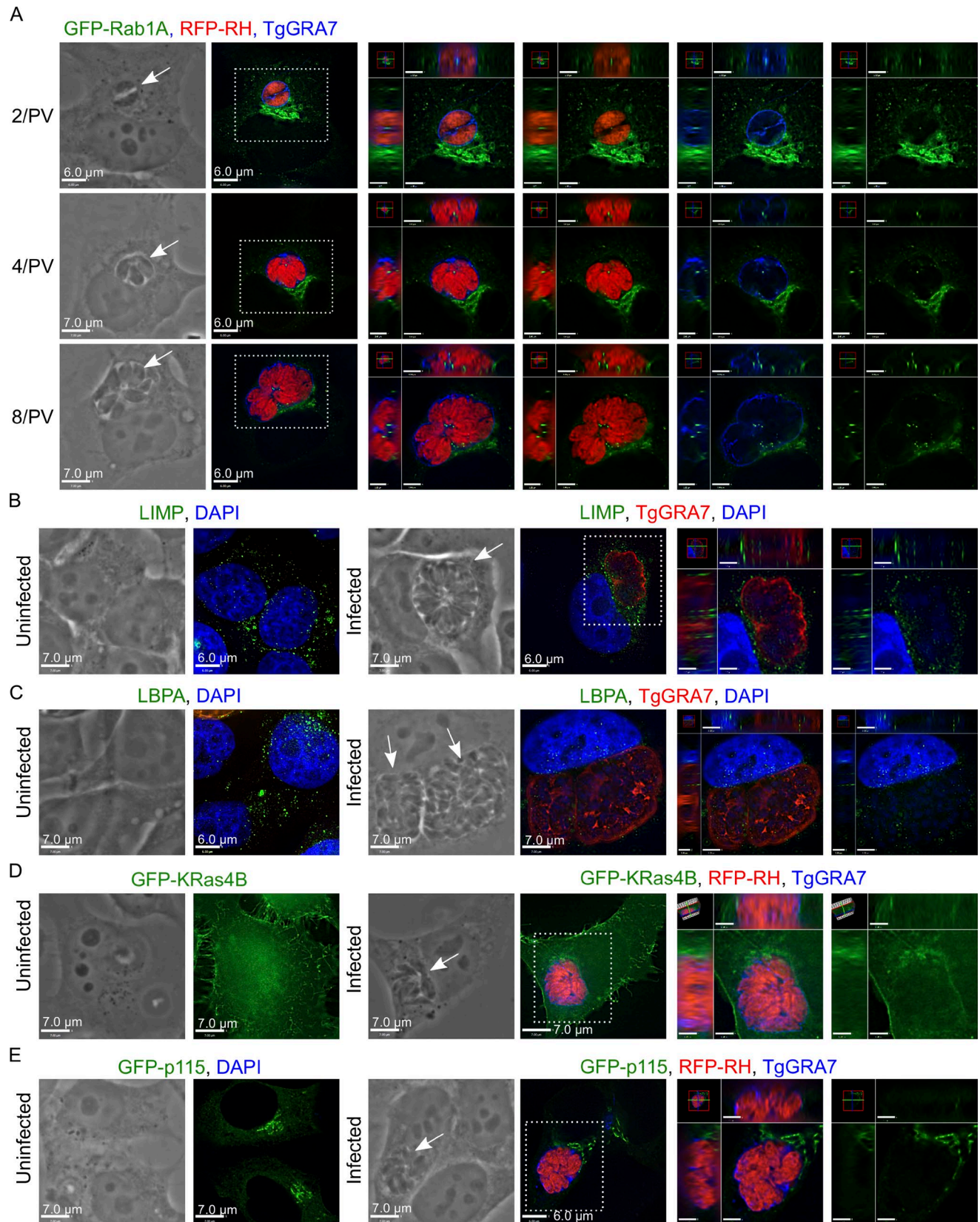


Figure S2. **Internalization of host proteins involved in vesicular trafficking and tethering.** (A) HeLa cells expressing GFP-Rab1A (green) were infected with RFP-RH (24 h) and immunostained for TgGRA7 (blue). PVs (arrows) with two, four, and eight parasites are shown. (B and C) HeLa cells infected with parasites (24 h) were immunostained for TgGRA7 (red) and LIMP (green, B) or lysobisphosphatidic acid (LBPA; green, C) and stained with DAPI (blue). (D and E) HeLa cells expressing GFP-KRas4B (green, D) or GFP-p115 (green, E) were infected with RFP-RH (24 h) and immunostained for TgGRA7 (blue). For all images, individual z-slices are shown; the boxed region is magnified in the orthogonal views.

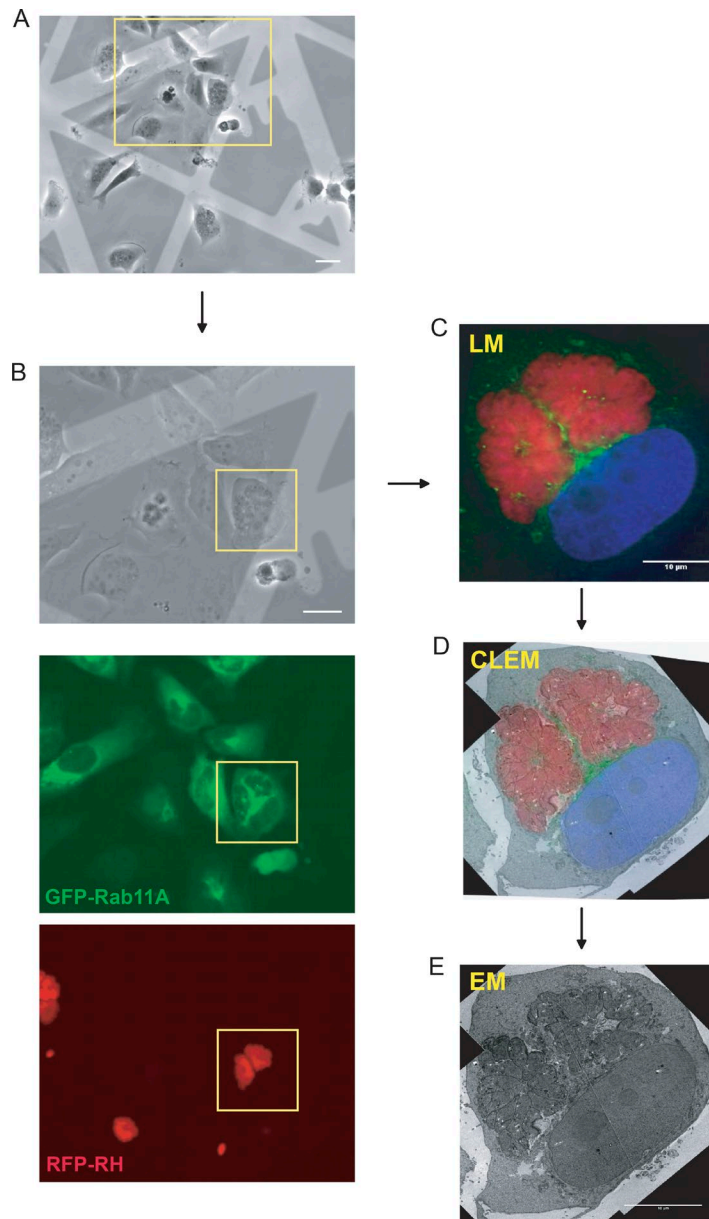


Figure S3. **CLEM of infected cells expressing GFP-Rab1.** (A) HeLa cells expressing GFP-Rab1A (green) were infected with RFP-RH (24 h), stained with DAPI (blue), and processed for CLEM. (A) Phase contrast image of cells (20x; bar, 30 μ m). (B) Phase contrast and fluorescence microscopy images (single optical z-slice) of the region within the yellow box in A (40x; bar, 30 μ m). (C–E) Merged fluorescence image of a single optical z-slice (C), overlay of the fluorescence and EM image (D), and EM image (E) of the region within the box from B. Bars, 10 μ m.

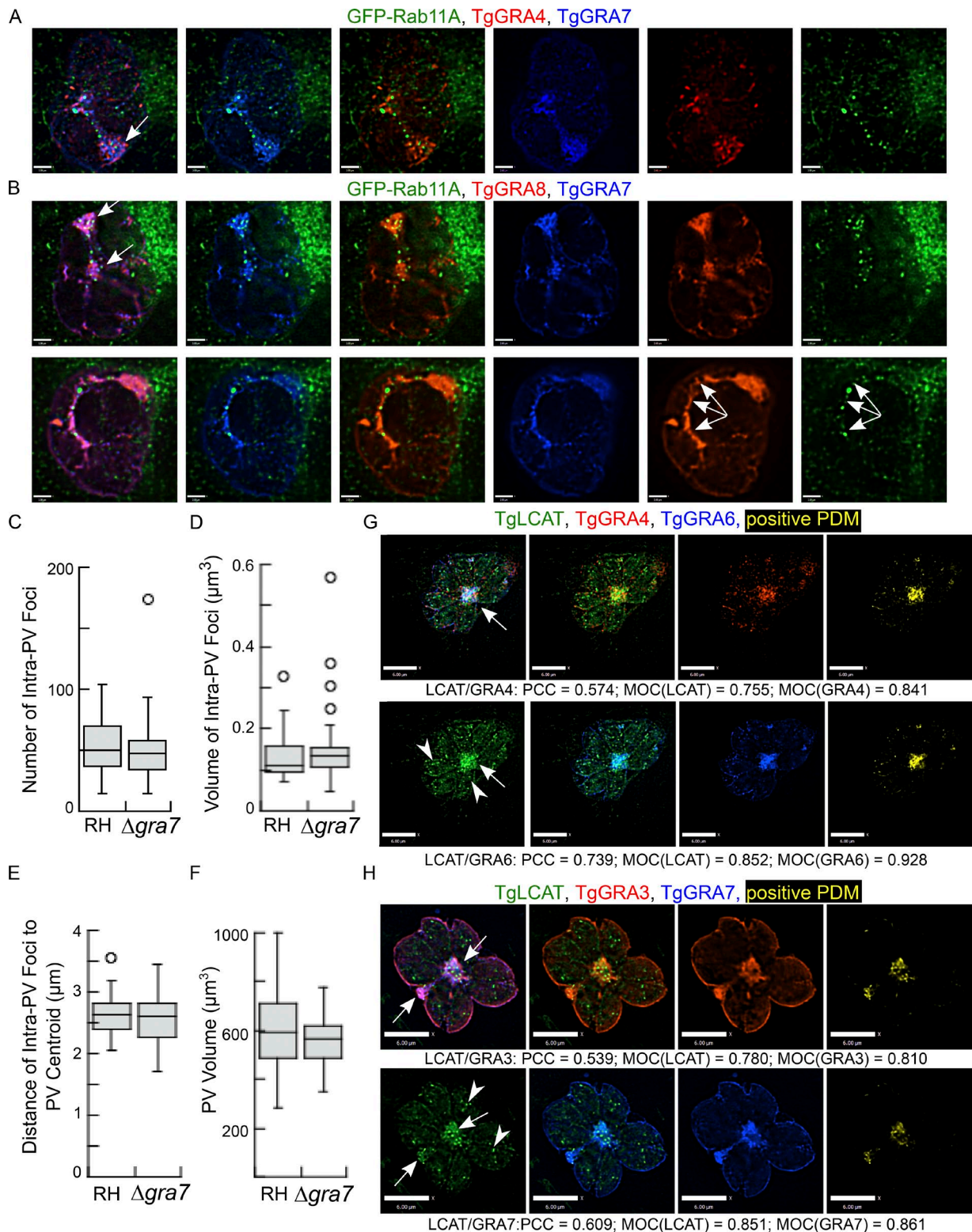


Figure S4. **Concentration of host GFP-Rab11A foci to the IVN containing TgLCAT and TgGRA7.** (A and B) Infected (24 h) VERO cells expressing GFP-Rab11A (green) were immunostained for TgGRA7 (blue) and TgGRA4 (red, A) or TgGRA8 (red, B). Arrows indicate concentrations of GFP-Rab11A with the IVN. The triple-headed arrow indicates GFP-Rab11A foci that localize along a strand of IVN. Bars, 2 μm . (C–F) GFP-Rab11A-expressing VERO cells infected with RH and Δgra7 parasites (24 h). The number (C), volume (D), and distance from the PV centroid (E) of intravacuolar GFP-Rab11A foci and the volume (F) of the PV were calculated and shown in box plots. There were no significant differences between the values as determined by a Student *t* test. (G and H) Infected (24 h) HFFs were immunostained for TgLCAT (green) and TgGRA4 (red) and TgGRA6 (blue, G) or TgGRA3 (red) and TgGRA7 (blue, H). Shown are fluorescent images of a single optical slice showing a positive PDM (yellow). PCC and MOC are calculated. Arrows and arrowheads point to TgLCAT localized with the IVN or in the parasite, respectively. Bars, 6 μm .

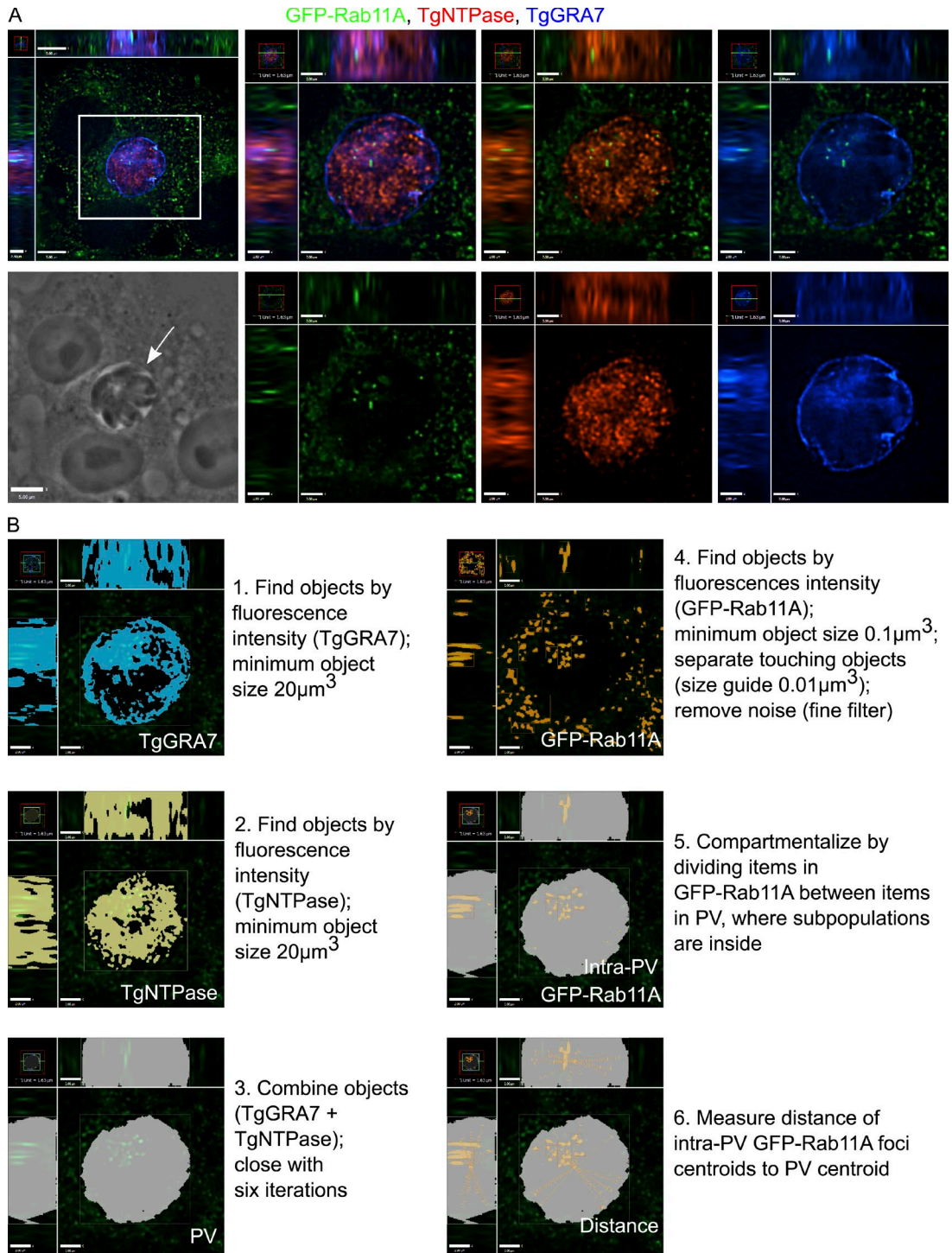


Figure S5. **Measurement protocol to assess intra-PV host GFP-Rab11A foci.** (A) Infected (24 h) VERO cells expressing GFP-Rab11A (green) were immunostained for TgNTPase (red) and TgGRA7 (blue) to detect the PV. Individual z-slices are shown, the boxed region is magnified in the orthogonal views and arrows indicate the PV. (B) A description of the steps of the Velocity measurement protocol with masks indicating the object detected (see Materials and methods). Bars: (A) 5 μm ; (B) 2 μm .